ELSEVIER
Available online at www.sciencedirect.com
SCIENCE DIRECT®
Physica C xxx (2003) xxx–xxx
PHYSICA C
www.elsevier.com/locate/physc

Suppression of *ab*-plane crack formation in single domain $YBa_2Cu_3O_x$ by uniaxial *c*-axis pressure

D. Shi [a,*], D. Isfort [b,c], X. Chaud [c], P. Odier [b], D. Mast [d], R. Tournier [b,c]

[a] *Department of Chemical and Materials Engineering, University of Cincinnati, Cincinnati, OH 45221-0012, USA*
[b] *Laboratoire de Cristallographie, CNRS, BP 166, F-38042 Grenoble Cedex 9, France*
[c] *Consortium de Recherches pour l'Emergence de Technologies Avancées, CNRS, BP 166, F-38042 Grenoble Cedex 9, France*
[d] *Department of Physics, University of Cincinnati, Cincinnati, OH 45221-0012, USA*

Received 19 May 2003; received in revised form 10 July 2003; accepted 25 August 2003

Abstract

A uniaxial *c*-axis pressure has been applied to $YBa_2Cu_3O_x$ (YBCO) single domain during a prolonged oxygenation experiment up to 72 h. It has been found that, due to this *c*-axis pressure, the local tensile stress responsible for *ab*-plane crack formation can be compensated effectively. The optical microscopy experimental results indicate that there is a sharp contrast in microstructure between the samples with and without *c*-axis pressure. The *ab*-plane cracks in the sample with *c*-axis pressure appear to be suppressed. X-ray diffraction results show that, for a 72 h-oxygen anneal, both samples with and without pressure are well oxygenated with equal orthorhombicity on the polished surfaces where the microstructures are studied. Also discussed is the mechanism of *ab*-plane crack suppression by the *c*-axis pressure.

1. Introduction

In $YBa_2Cu_3O_x$ (YBCO) single domain, *ab*-plane cracks inevitably form due to large stresses induced during the tetragonal (T) to orthorhombic (O) phase transformation [1–3]. Therefore, crack formation is inherently a structure-related behavior governed by oxygen diffusion. With these cracks in the matrix of the crystal, the integrity of the domain structure is severely altered making its usefulness limited. For instance, the mechanical strength of the YBCO single domain is significantly reduced and the materials easily cleave along the *ab*-plane cracks. In magnetic levitation, these cracks interfere with the induced currents; thus lower the trapped field and levitation force. In fundamental studies, these imperfections make it difficult to control the physical parameters that are needed for modeling.

One of the novel applications is in the RF wireless telecommunications. The recent development of extremely low loss RF components using high temperature superconductors (HTS) such as YBCO has succeeded in achieving the extremely low surface resistance at the appropriate cellular frequencies. The current technologies in fabrication of HTSs for RF applications have been primarily the thin film approaches that can produce

* Corresponding author. Tel.: +1-513-556-3100; fax: +1-513-556-1004.
E-mail address: donglu.shi@uc.edu (D. Shi).

0921-4534/$ - see front matter © 2003 Elsevier B.V. All rights reserved.
doi:10.1016/j.physc.2003.08.011

well-textured $YBa_2Cu_3O_x$ materials with extremely low surface resistance [4,5]. The recent development in seeded melt growth (SMG) of YBCO has shown great promise in the fabrication of RF components with superb RF properties. Not only has the surface resistance of the SMG reached a value comparable to those of thin films, great advantages in utilizing this HTS material also lie in its suitability for mass production, easy control of device geometry, and low cost.

One of the concerns for single domain YBCO is that it inherently contains these *ab*-plane microcracks. As RF waves travel through the surfaces, great loss can take place at these cracked regions. Note that the microwaves only penetrate about 1μm depth on the surface, therefore these surface defects become more critical in reducing the RF losses and device design. There have been, however, a few systematic studies so far to investigate the effective methods that can prevent these surface cracks.

Suasmoro was the first to use in situ ultrasonic wave attenuation to probe the microstructure of YBCO ceramic polycrystals [6]. He concluded, based on the ultrasonic data, that the microcracks formed in the tetragonal phase region where oxidation was taking place. Diko had made an extensive analysis on the behavior of microcracks in textured YBCO [7]. He discussed on the origin of these cracks: i.e., whether these are growth defects or oxygen annealing defects. Growth defects were found parallel to the *ab*-planes due to a growth gap generated by inclusions of 2 1 1 particles during crystallization. Diko attributed the microcracking phenomena to a thermal expansion stress between oxidized and non-oxidized zones. The oxygenation was thought to be a combination of oxygen volume diffusion, microcracking, and oxygen penetration along the cracks.

In a recent study by Shi et al. on crack formation and propagation in YBCO single domain, they concluded that, during oxygenation, the phase transition has created a large volume stress that is responsible for rapid crack propagation in the YBCO crystal [8]. Due to severe contraction in the *c*-direction, the crystal under goes a compressive deformation. However the structurally isotropic 2 1 1 particles prevent the compressive deformation in some local areas especially near the 2 1 1 particles, therefore diverting the compressive stress to tensile stress. As the tensile stress reaches the critical value, the cracks begin to propagate inwardly in the crystal. The T-to-O phase boundary provides the driving force for the propagation of the cracks. Since the T-to-O transition is oxygen diffusion controlled, the kinetics of crack propagation is dictated by the rate of oxygen diffusion. After the oxygen content is homogeneously established in the sample, there is no further driving force for the propagation of cracks.

Based on these studies, in this paper, we report on a new method by which the *ab*-plane crack formation was suppressed by applying a uniaxial *c*-axis pressure to the single domain directly. Both optical microscopy and X-ray diffraction results of the annealed samples are presented. The mechanism on suppression of crack formation is discussed.

2. Experimental

The seeded melt growth (SMG) method was originally developed for the purpose of producing large domains for various engineering applications [9–12]. The single domain samples were disc shaped pellets (20 mm in diameter and 15 mm in height). We used precursors of 70 wt% $YBa_2Cu_3O_x$, 30 wt% Y_2BaCuO_5, and 0.15 wt% Pt. These powders were thoroughly mixed and uniaxially pressed at 100 MPa into a disc shaped green pellet of 35 g. The green pellet was sintered in air at 930 °C for 24 h. A $SmBa_2Cu_3O_x$ single domain was used as seed having a dimension of $2\times2\times1.5$ mm^3. The seed was put on the top of the green pellet before the growth process. The green pellet was placed on an alumina plate with an intermediate layer of Y_2O_3 powder to avoid liquid spreading on the interior surfaces of the furnace. A sintered thin plate consisting of a mixture of $YbBa_2Cu_3O_x$ and $YBa_2Cu_3O_x$ was also used between the green pellet and the Y_2O_3 layer. This substrate was found necessary to avoid parasitic grain growth from the bottom. After the completion of the domain growth, the sample was cooled in nitrogen gas to prevent the phase transformation from the tetragonal to orthorhombic structure. In this way, the sample is free of *ab*-plane crack formation. The details about the YBCO single domain growth can be found in Refs. [13–16].

In this experiment, a 2.5-mm-thick YBCO disc of 20 mm diameter was sliced along the *ab*-plane from the crack-free single domain pellet for the pressure experiment. The virgin sample had the tetragonal phase as it was cooled in nitrogen gas. The disc sample was cut, parallel to the *c*-axis, into two pieces with the facing surfaces polished down to 1 μm for optical microscopy studies. The mirror-image surfaces were used to ensure that the studied regions were adjacent to each other. The pressure vise was a commercial flange made of stainless steel as shown in Fig. 1. The flange diameter was 34 mm with a thickness of 7.2 mm. As shown in Fig. 1b, the disc sample was sandwiched between two flanges tightened with screws. Before tightening the screws, the flanges were placed in a hydraulic press for achieving a uniform force along *c*-axis. As the hydraulic pressure reached 15 MPa, six 4.2 mm screws were hand-tightened. To ensure a uniform pressure, the top and bottom surfaces of the disc sample were polished by a special device making these surfaces parallel to each other. Note that a device that has resulted in a more uniform force on Bi2223 has been reported in a previous work [17]. To study the effect of pressure on the crack behavior, we are in the process of designing a better device and monitor the pressure at the annealing temperatures.

Both samples (each half) with and without pressure were annealed together in flowing oxygen at 400 °C for 18, 48 and 72 h. At each annealing interval, the samples were cooled to room temperature and used for optical microscopy and X-ray diffraction (XRD). After these studies, the samples were put back into the furnace for a prolonged oxygenation under the same condition up to 72 h.

A thin layer from the polished surfaces of the oxygenated samples (with and without pressure) was powdered and analyzed by X-ray diffraction (XRD) using a Siemens diffractometer (D5000) operating in transmission mode with Cu Kα radiation.

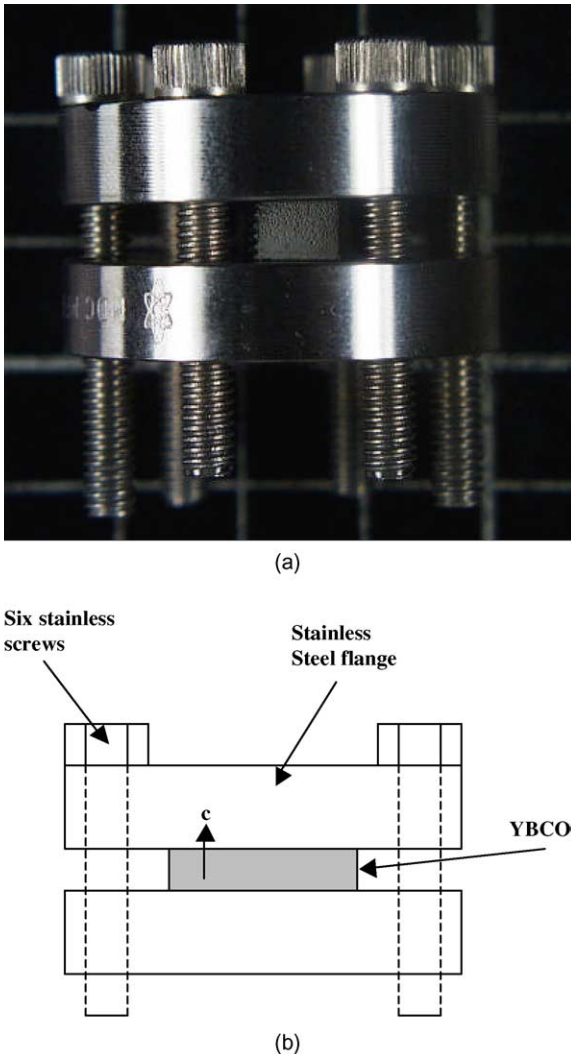

Fig. 1. (a) A photograph showing the stainless steel pressure vise and (b) schematic diagram showing the application of uniaxial *c*-axis pressure.

3. Results

Fig. 2a shows the microstructure of the as-grown YBCO single domain. Due to flowing nitrogen during cooling, the YBCO phase remains un-oxygenated with a tetragonal structure. No cracks are observed in this sample. However, after the sample was treated in flowing oxygen at 400 °C for 18 h, microcracks formed as shown in Fig. 2b, which have been typically seen in many previous

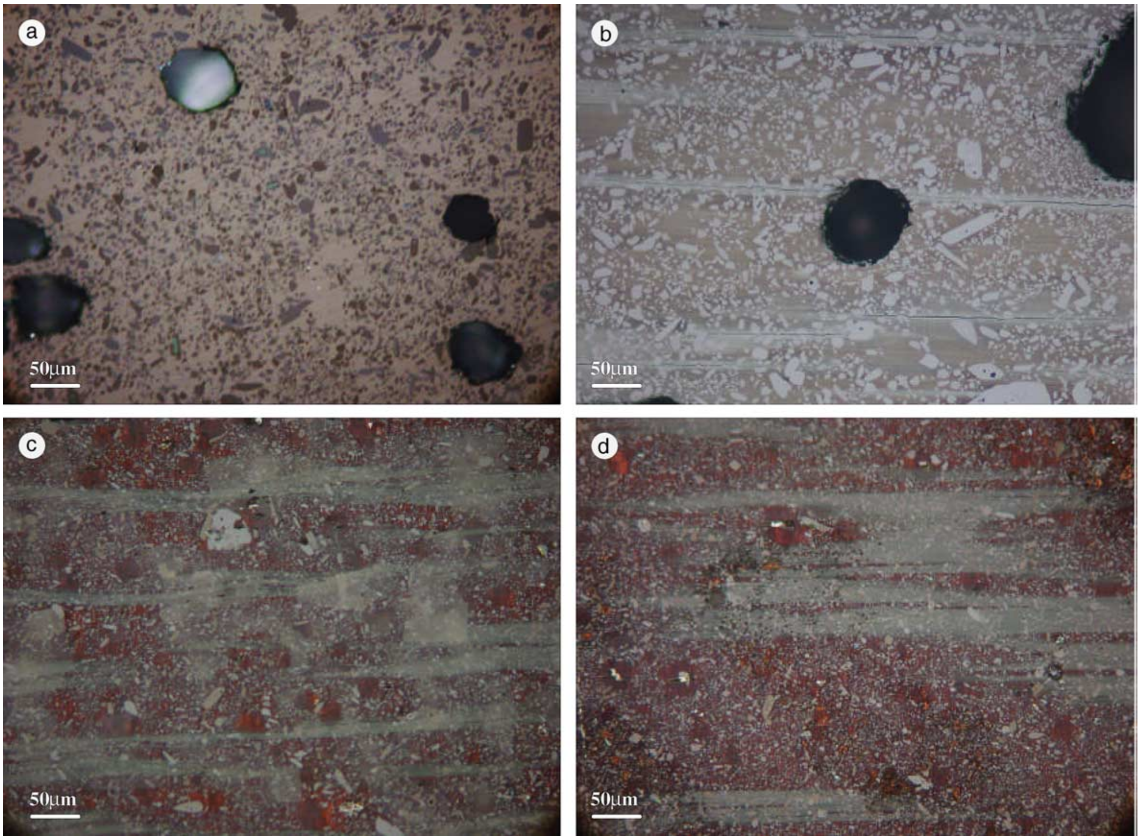

Fig. 2. (a) Optical micrograph showing the microstructure of the as-grown single domain, (b) optical micrograph showing the microstructure of the sample annealed at 400 °C for 18 h without pressure, (c) optical micrograph showing the microstructure of the sample annealed at 400 °C for 18 h with the *c*-axis pressure, and (d) the same as in (c) but another area.

studies. Note that there are regions which have different contrast with the matrix in which the cracks are visible. These regions are assumed to be more oxygenated than the matrix. Upon crack formation, oxygen diffusion becomes more rapid along the crack. As the oxygen diffuses into the sample along the *ab*-planes, these microcracks also propagate into the interior of the domain structure at a rate that is comparable to that of oxygen diffusion. However, in this study we only focused on the *polished surfaces* of the annealed samples with and without pressure. The crack formation inside the matrix of the sample is being investigated in a more detailed study. Fig. 2c shows the counterpart of the sample that was annealed under the *c*-axis pressure. Regions with light contrast, similar to those shown in Fig. 2b, are observed. In these regions, no visible cracks were observed with optical microscopy. Fig. 2d shows another area of the sample. Again it indicates a quite homogeneous microstructure throughout the entire sample.

Fig. 3 shows the microstructures of the samples annealed for 48 h with and without *c*-axis pressure. Quite similar microstructural behaviors shown in Fig. 2 have been observed in these pictures (e.g. with *c*-axis pressure, no microcracks are observed). We found the identical microstructural differences between the samples with and without *c*-axis pressure as shown in Fig. 4. Up to an annealing time of 72 h, the sample with pressure remains uncracked as can be seen in this figure. As these *ab*-plane cracks were initiated by oxygen diffusion, for samples with *c*-axis pressure applied we needed

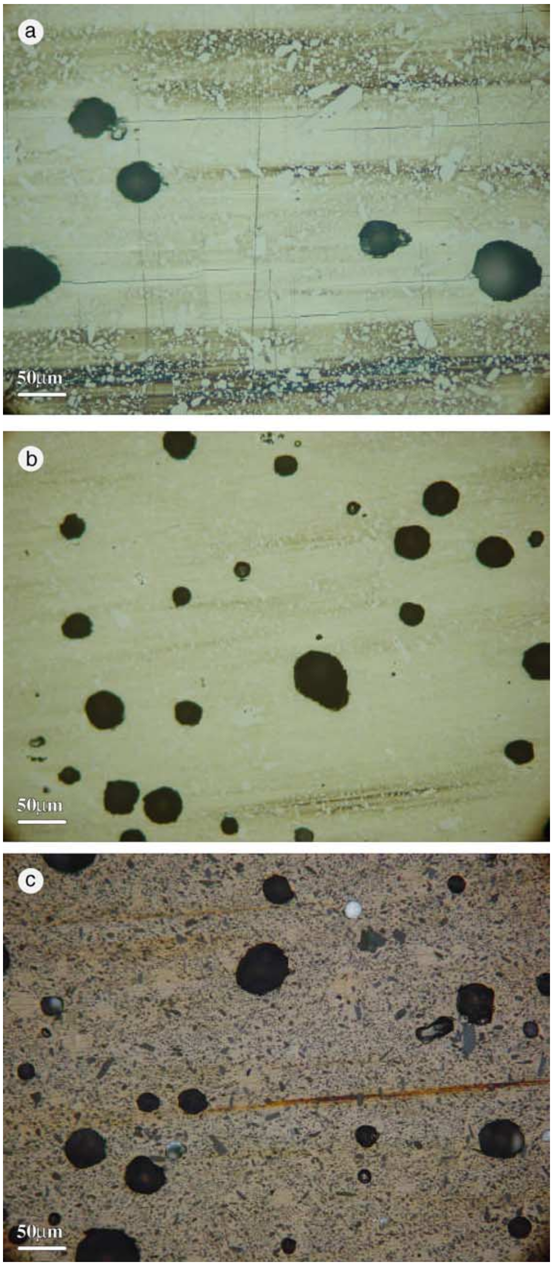

Fig. 3. (a) Optical micrograph showing the microstructure of the sample annealed at 400 °C for 48 h without pressure, (b) optical micrograph showing the microstructure of the sample annealed at 400 °C for 48 h with the *c*-axis pressure, and (c) the same as in (b) but another area.

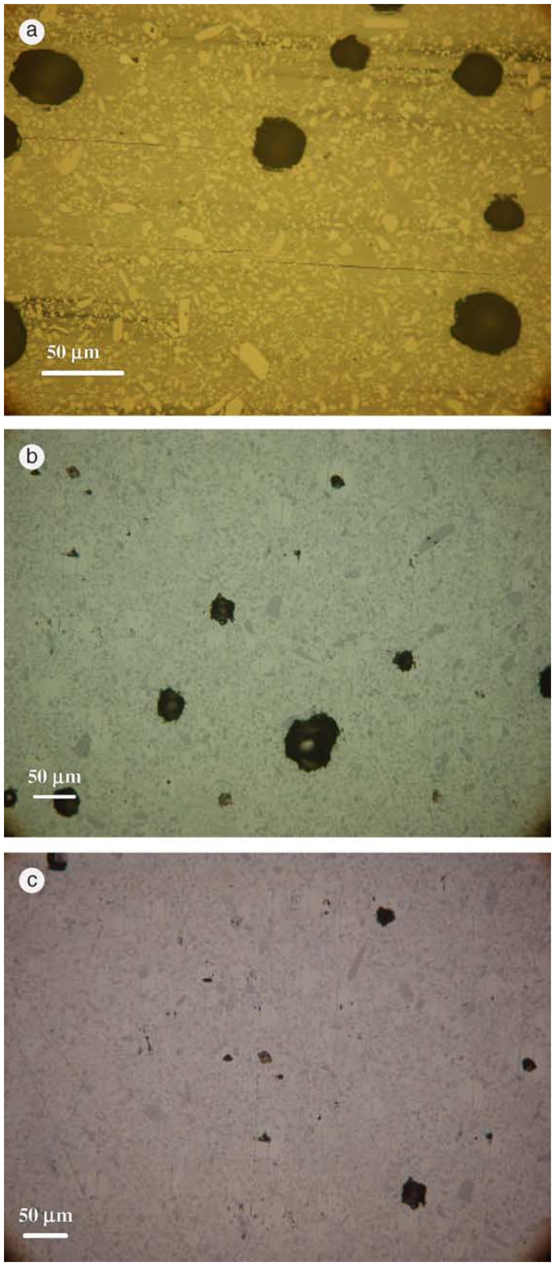

Fig. 4. (a) Optical micrograph showing the microstructure of the sample annealed at 400 °C for 72 h without pressure; (b) optical micrograph showing the microstructure of the sample annealed at 400 °C for 72 h with the *c*-axis pressure, and (c) the same as in (b) but another area.

to examine the oxygen content in these samples with and without pressure.

To determine the oxygen content and the orthorhombicity of the annealed samples, XRD was carried out on both polished surfaces for the 72 h-annealed samples with and without pressure. Small portions of material were taken from these sample surfaces (i.e. the sample with pressure and the sample without pressure) for the XRD powder diffraction. The spectrum was recorded in the angular range 10–100° in 2θ and the lines of $YBa_2Cu_3O_x$ phase were indexed according to the Pmmm space group. Only the lines that did not overlap with those of the Y_2BaCuO_5 phase (2 1 1) were taken into account for calculation of the unit cell parameters by a least square refinement method (Cellref program). We then used 25 lines, which were sufficient to provide accurate indexing. In a second attempt we mounted the 72 h-annealed samples directly on a four-circle goniometer. We registered the first $h00$ and $0k0$ reflections and used the Nelson–Riley procedure to extrapolate a and b values [18]. In this procedure, the calculated parameters for each set of data were plotted versus $\cos^2\theta/\sin\theta$ (Fig. 5). The extrapolation to zero gives a very good approximation of the cell parameter. Both methods agree to point out that these samples have the identical lattice parameters (see Fig. 5a and b), indicating that they are fully oxygenated and have an orthorhombic structure at the *polished surfaces*.

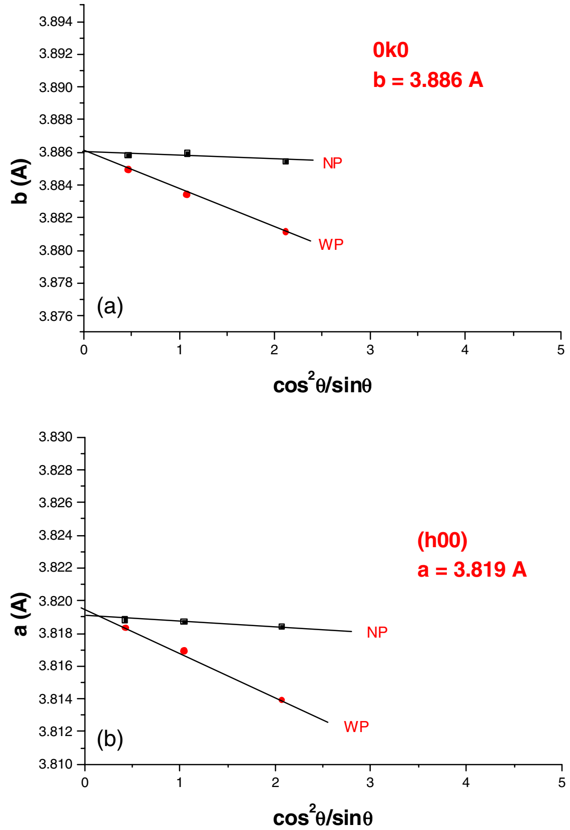

Fig. 5. (a) Lattice parameter b versus $\cos^2\theta/\sin\theta$ for both samples with and without pressure annealed at 400 °C for 72 h and (b) Lattice parameter a versus $\cos^2\theta/\sin\theta$ for both samples with and without pressure annealed at 400 °C for 72 h.

4. Discussion

Applications of pressure on oxide superconductors have been reported in the past for achieving various unique properties. Zhu et al. have reported a compressive anneal processing of Bi2223 superconducting tapes for enhancement of texture [17]. During oxygenation, tetragonal to orthorhombic phase transition takes place that generates volume stresses due to dimensional changes of the unit cell. To accommodate the volume stresses, twinning occurs as have been well observed in previous studies [1–4]. To study the effects of twins on various physical properties such as flux pinning and superconducting fluctuations, moderate *ab*-plane uniaxial pressure was applied to remove the twin boundaries [19–21]. However, we believe that, it is the first time that a c-axis pressure has been applied to suppress *ab*-plane crack initiation and propagation.

The *ab*-plane crack formation has extensively been studied previously [22,23]. During oxygen diffusion from the surface of the YBCO sample, an oxygen gradient is created. As a result of c-axis contraction, a tensile stress is created in the outer regions of the sample. This strain profile in the oxygenated layer will cause cracking parallel to *ab*-plane with cracks apparent at the sample surface [22]. The 2 1 1 particles in the YBCO single domain can also contribute to the *ab*-plane cracks [23]. This local tensile stress will initiate cracks along *ab*-planes and the level of this stress depends on the size of 2 1 1 particles, presumably, the larger the particle, the higher the stress. From our microstructural observation the particles size range from submicron up to 20 μ with an average size of 2 μm and a few large 2 1 1 particles resulted from peritectic reaction, therefore can generate stresses in a wide range. As the YBCO single domain contains a high concentration of 2 1 1 particles (30 wt% in initial concentration), they will hinder the *c*-axis change and create a local tensile stress near themselves. The *c*-axis variation with annealing time was previously published by Shi et al. [24]. Such *ab*-plane cracks near the 2 1 1 particles have been commonly observed [22–24]. Therefore to compensate this local tensile stress that is responsible for *ab*-plane cracks, a uniaxial *c*-axis pressure can be applied by using the simple vise shown in Fig. 1. As the vise applies the pressure along the *c*-axis, the single domain will deform elastically although moderately. The *c*-axis pressure would confine the crystal deformation along the *c*-axis during oxygenation. For a crack to initiate, local tensile stress is required. The *c*-axis pressure can provide an effective counter pressure that compensates this local tensile stress. In this way, the crack formation is suppressed. However, in this initial experiment, it is difficult to quantitatively determine the local crack tip stress and the counter force from the uniaxial pressure applied. More detailed experiments addressing these critical stresses are underway.

The *ab*-plane crack nucleation and propagation have been previously studied by Shi et al. [24]. In their experiments, Young's modulus experiments were carried out to study the kinetics of *ab*-plane crack propagation in single domain $YBa_2Cu_3O_x$ (YBCO) during a prolonged oxygen heat treatment at 400 °C up to 188 h. It was found that the modulus value experiences a rapid fall between the annealing time of 48 and 96 h, indicating the kinetics of crack propagation in the sample matrix. For 72 h annealed the sample, based on the results of this previous work, the *ab*-plane cracks have propagated through the entire cross section along the *ab*-plane. With the confinement of the *c*-axis pressure, not only can the crack initiation be significantly repressed, but also the kinetics slowed down. However, in this experiment, our experiments are only focused at the polished surfaces of annealed samples with and without *c*-axis pressure. The effects of *c*-axis pressure on crack propagation in the matrix of the single domain are currently being carried out.

5. Summary

In order to suppress *ab*-plane crack formation, uniaxial *c*-axis pressure is applied to the YBCO single domain. In a prolonged oxygen anneal, this *c*-axis pressure has effectively suppressed the formation of the *ab*-plane cracks on the *polished surfaces*. These results indicate that by applying pressure along the *c*-axis, local tensile stresses responsible for initiating *ab*-plane cracks can be compensated effectively; thereby providing a unique method for eliminating cracks in the YBCO single domain.

Acknowledgement

One the of authors (D. Shi) is grateful to the financial and technical support from Laboratoire de Cristallographie and Consortium de Recherches pour l'Emergence de Technologies Avancées, CNRS, Grenoble, France.

References

[1] D. Shi, D.W. Capone II, K.C. Goretta, K. Zhang, G.T. Goudey, J. Appl. Phys. 63 (1988) 5411.
[2] D. Shi, K. Zhang, D.W. Capone II, J. Appl. Phys. 64 (1995) 1988.
[3] D. Shi, Phys. Rev. B. 39 (1989) 4299.
[4] J.D. Jorgensen, Jpn. J. Appl. Phys. 26 (1987) 2017.
[5] T. Siegrist, S. Sunshine, D.W. Murphy, R.J. Cava, S.M. Zahurak, Phys. Rev. B 35 (1987) 7137.
[6] Suasmoro, Ph.D. dissertation, 1992.
[7] P. Diko, N. Pelerin, P. Odier, Physica C 247 (1995) 169.
[8] D. Shi, P. Odier, A. Sulpice, D. Isfort, X. Chaud, R. Tournier, P. He, R. Singh, Physica C 384 (2003) 149.
[9] D. Shi, W. Zhong, U. Welp, S. Sengupta, V. Todt, G.W. Crabtree, S. Dorris, U. Balachandran, IEEE Trans. Magn. 5 (1994) 1627.
[10] M. Murakami, M. Morita, N. Koyama, Jpn. J. Appl. Phys. 28 (1989) L1125.
[11] V.R. Todt, S. Sengupta, D. Shi, J. Hull, P.R. Sahm, P.J. McGinn, R. Peoppel, J. Electron. Mater. 23 (1994) 1127.
[12] D. Shi et al., Physica C 246 (1995) 253.

PHYSC 51054
8 October 2003 Disk used
ARTICLE IN PRESS
No. of Pages 8, DTD = 4.3.1

[13] P. Gautier-Picard, X. Chaud, E. Beaugnon, A. Erraud, R. Tournier, Mater. Sci. Eng. B 53 (1998) 66.
[14] P. Gautier-Picard, E. Beaugnon, X. Chaud, A. Sulpice, R. Tournier, Physica C 308 (1998) 161.
[15] X. Chaud, D. Isfort, E. Beaugnon, R. Tournier, Physica C 2413 (2000) 341.
[16] K. Conder, Mater. Sci. Eng. 32 (2001) 41.
[17] Zhu et al., Supercond. Sci. Technol. 12 (1999) 640.
[18] H.P. Klug, L.E. Alexander, X-ray Diffraction Procedures for Polycrystalline and Amorphous Materials, second ed., John Wiley and Sons, 1974.
[19] R. Liang, D.A. Bonn, W.N. Hardy, Phys. Rev. Lett. 76 (1996) 835.
[20] M. Pissas, E. Moraitakis, G. Kallias, Phys. Rev. B. 62 (2000) 1446.
[21] U. Welp, J.A. Fendrich, W.K. Kwok, G.W. Crabtree, B.W. Veal, Phys. Rev. Lett. 76 (1996) 4809.
[22] P. Diko, G. Krabbes, Supercond. Sci. Technol. 16 (2003) 90.
[23] D. Isfort, X. Chaud, R. Tournier, G. Kapelski, Physica C 390 (2003) 341.
[24] D. Shi, P. Odier, A. Sulpice, D. Isfort, X. Chaud, R. Tournier, P. He, R. Singh, Physica C 384 (2003) 149.